DOI 10.1007/s11182-021-02466-4
Russian Physics Journal, Vol. 64, No. 6, October, 2021 (Russian Original No. 6, June, 2021)

PHYSICAL AND MECHANICAL BEHAVIOR OF ICE UNDER DYNAMIC LOADING

A. I. Potekaev, G. N. Parvatov, V. V. Skripnyak, and V. A. Skripnyak UDC 539.2:621.311.25

The physical and mechanical behavior of ice is studied by the example of the Ih ice phase using the method of numerical simulation in a computational model of damaged medium in order to describe the common factors of deformation and fracture of ice under dynamic loading. The development of inelastic strains and the evolution of damage accumulation under high-rate loading are described by the Johnson–Holmquist (JH2) damage model. The computations are performed in a 3D formulation using an explicit second-order accuracy difference scheme. The computational model is calibrated with respect to the experimental data obtained in a wide range of strain rates using the Kolsky method and in the experiments on ice loading with plane shock waves. It is shown that the proposed physical-mechanical concepts and the model of ice behavior under dynamic loading proposed in this study provide both qualitative and quantitative agreement of the results of mechanical behavior of Ih ice with the available experimental data in a range of pressures from 0 to 150 MPa, at the temperatures from 193 to 273 K, and a range of strain rates from 0 to 2000 1/s. This evidences of the validity of the concepts used and allows predicting the ice behavior under dynamic loads.

Keywords: ice, mechanical behavior of ice, high strain rates, fracture, dynamic compressive strength.

INTRODUCTION

The physical and mechanical behavior of ice under loading (especially dynamic) is very important for applied problems, therefore the physical and mechanical properties of solid water phases have been studied since early 20th century. The experimental studies demonstrated that Ih freshwater ice at the pressures of up to 2 GPa is found in 17 different crystallographic phases characterized by different specific volumes, temperatures and values of internal heat of melting [1]. The uttermost interest is caused by the mechanical behavior of a water ice modification in a stable hexagonal phase Ih, which persists at a pressure of up to 150 MPa in a temperature range from 193 to 273 K [1–11].

The elaboration of physical-mechanical concepts and models aimed at a description of the mechanical behavior of Ih water ice under dynamic impact in recent years have been pursued in several directions [2–14]. There are phenomenological macromechanical models developed for the description of ice response to dynamic impacts, using classical dynamic fracture criteria [2, 3]. There has been an active development of a model of mechanical behavior of ice within the frame of the continuum damage mechanics [4]. The experimental research has shown that the mechanical behavior of Ih ice, including its fracture modes, is strain rate dependent [2–9]. In view of this fact, in order to get an insight into the mechanical behavior of ice and to predict it under dynamic impacts, the concepts are being developed which include into consideration its viscoplasticity and fracture as a result of crack nucleation and growth [5, 10–12]. The multi-level models developed at present include the crystallite size and the characteristic ice structure at the mesoscopic level [13,14]. Despite the active development of the concepts and models of mechanical behavior of Ih ice

National Research Tomsk State University, Tomsk, Russia, e-mail: potekaev@spti.tsu.ru; georgpa@yandex.ru; skrp2012@yandex.ru; skrp2006@yandex.ru. Translated from Izvestiya Vysshikh Uchebnykh Zavedenii, Fizika, No. 6, pp. 89–94, June, 2021. Original article submitted December 10, 2020.

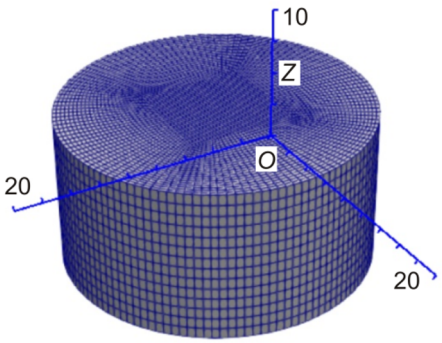

Fig. 1. Simulated sample (computational domain) of water ice.

under dynamic impacts, the understanding of processes of high-rate strain and fracture dynamics is far from the level necessary for making a proper forecast.

Of critical importance is the necessity of understanding, describing and predicting the ice behavior under dynamic loading in the temperature range of 193–273 K, which appears in the prediction of high-rate interaction of ice particles with the aerospace structures, land and water transport systems, gas turbine blades of aircraft engines and engine superchargers, etc.

The purpose of this work is to study the mechanical behavior of ice to shock-pulse impact by simulating it in a continuum damage model using Ih ice as an example.

MODEL APPROXIMATIONS AND METHODS

The mechanical behavior of ice under dynamic loading is studied by the example of the Ih ice phase using the method of numerical simulation in an approximation of a damaged medium. The mechanical behavior of ice under dynamic loading is described within the frame of the Johnson–Holmquist approach [15].

For this purpose, we constructed a computational model of mechanical behavior of Ih under dynamic impacts. To refine the numerical parameter values of the mechanical behavior of ice, considered as a damage medium (*MAT_110) [16], we used the experimental data in the constitutive equation [6].

The simulated ice sample was shaped as a cylinder (Fig. 1) with a diameter of $2r$ = 20 mm and a thickness of h = 10 mm, which corresponded to the geometrical characteristics of the sample in the experiment [6].

The finite-element model of the sample (Fig. 1) consisted of 54 000 hexahedral Lagrange elements corresponding to the ELFORM1 elements in the LS DYNA package (ANSYS Inc.) [16]. The contact between the surfaces of interacting fragments, formed in the course of the model sample fracture, was set using the *ERODING_SINGLE_SURFACE model [16]. In the model, the sample was placed between two rigid walls, one of which was thought to be immobile in space, which is described by the boundary conditions in *RIGID_WALL_ GEOMETRIC_FLAT. The second wall was mobile, the options of its boundary conditions were set by *RIGID_WALL_GEOMETRIC_FLAT_MOTION. Free boundary conditions were set on the lateral surface of the sample.

The shape and amplitude of the exciting pulse were selected in accordance with the experimental data [6]. When the wall was moving along the *OZ* direction (Fig. 1) at a rate corresponding to the compressive pulse, the model sample volume was compressed and fragmented as a result of damage nucleation and growth.

The elastic behavior of polycrystalline Ih water ice is characterized by moderate anisotropy [15], therefore the ice was treated as an isotropic damageable medium. The dependence of elastic moduli of Ih ice on temperature in the temperature range from 193 to 273 K was described by the phenomenological relations [17–19]

$$E = E_{Tm} + k_E (T_m - T)\,,\ G = G_{Tm} + k_G (T_m - T)\,,\ \nu = \nu_{Tm} + k_\nu (T_m - T)\,, \quad (1)$$

where ν is the Poisson's ratio, E is the Young modulus, $E_0 \approx 10$ GPa is the phenomenological constant for Ih ice, $E_{T_m} = 8.93$ GPa, $k_E = 0.012$ GPa K^{-1}, T_m is the ice melting temperature, G is the shear modulus, $G_{T_m} = 3.31$ GPa, $k_G = 0.0045$ GPa K^{-1}, $\nu_{T_m} = 0.308$, $k_\nu = 7\ 10^{-5}$ K^{-1}. At the temperatures close to the ice melting temperature of 273 K, the Young modulus is 8.93 GPa. These numerical values of the coefficients were obtained by approximating the experimental data by other authors [12–14] using formulas (1).

The mechanical response of Ih ice on the intense pulse action in the pressure range before the phase transition [2, 20–22]

$$p = k_1 \mu + k_2 \mu^2 + k_3 \mu^3 \text{ during compression,}$$

$$p = k_1 \mu \text{ during tension,} \tag{2}$$

where $p = -(1/3)\sigma_{kk}$ is the pressure, σ_{ij} are the stress tensor components, $\mu = \rho/\rho_0 - 1$, ρ is the mass density, ρ_0 is the mass density of ice at a temperature close to the melting temperature.

Numerical values of the coefficients $k_1 - k_3$ in the equations of state (2) were determined by approximating the experimental shock adiabat [16]. The values of the Hugoniot elastic limit (HEL), pressure (P_{HEL}) and yield stress σ_{HEL} at the HEL can be derived using the following formulas [16, 21]:

$$\text{HEL} = k_1 \mu_{HEL} + k_2 \mu^2_{HEL} + k_3 \mu^3_{HEL} + (4/3) G[\mu_{HEL}/(1 + \mu_{HEL})], \tag{3}$$

$$P_{HEL} = k_1 \mu_{HEL} + k_2 \mu^2_{HEL} + k_3 \mu^3_{HEL},\ \sigma_{HEL} = 1.5(\text{HEL} - P_{HEL}),$$

where $\mu_{HEL} = \rho_{HEL}/\rho_0 - 1$, ρ_{HEL} is the mass density at the Hugoniot elastic limit and G is the shear modulus.

The equivalent stress σ_{eq} in the case of inelastic deformation of Ih ice would be determined within the frame of the model by the expression [17]

$$\sigma_{eq} = \sigma_i^* - D\left(\sigma_i^* - \sigma_f^*\right), \tag{4}$$

where $\sigma_{eq} = [(3/2)\sigma_{ij}\sigma_{ij} - (3p)^2]^{1/2}$ is the equivalent stress, D is the ice damage parameter, $\sigma_i^* = a(p^* + t^*)^n (1 + c \ln \dot{\varepsilon}^*)$ is the ice flow stress in the undamaged state, $\sigma_f^* = b(p^*)^m (1 + c \ln \dot{\varepsilon}^*) \le SF_{max}$ is the strain resistance of local volumes of fractured ice under compression, $t^* = T/P_{HEL}$, $p^* = p/P_{HEL}$, a, b, m, n, c are the material constants, T is the maximum tensile strength, ε* is the normalized rate of inelastic deformation, SF_{max} is the constant characterizing the maximum stress of the local volumes of the fractured medium. Relation (4) includes the effect of ice damage within the frame of the approach of the continuum damage mechanics [23–25]. The medium is damaged as a result of distributed cracking inside the loaded ice volume under dynamic impact, which is consistent with the experimental observations [2].

The ice damage parameter D is determined by the following relation [15]:

$$D = \sum \frac{\Delta\varepsilon^p}{\varepsilon_f^p}, \tag{5}$$

where $\Delta\varepsilon^p$ is the increment of the equivalent inelastic strain in a 3D-mesh element, $\varepsilon_f^p = d_1(p^* + t^*)^{d_2}$, d_1 and d_2 are the constants for ice, which characterize the processes of structure damage nucleation and accumulation in the mesh element.

The simulations were carried out using the solver of the LS DYNA software code (ANSYS Inc.) [16].

RESULTS AND DISCUSSION

Numerical values of the coefficients in equations (2)–(4) were found by two methods: by a direct approximation of the available experimental [20–22] and from the condition of achieving an agreement of the calculation with the experiment on the macroscopic parameters of the sample response to dynamic actions. PThe results of simulation of high-rate compression of a cylindrical ice sample using the LS-DYNA solver [16] were compared with the experimental data [6]. As a result, the numerical parameter values were found, which provided an agreement of the simulation results with the experiment

$$\rho_0 = 8\cdot 10^2\ \text{kg}\cdot\text{m}^{-3},\quad G = 3.5\ \text{GPa},\quad a = 0.88,\quad b = 0.1,\quad c = 0.0001,\quad m = 0.25,\quad n = 0.258,$$

$$\dot{\varepsilon}_0 = 1.0\ \text{s}^{-1},\quad T = 0.0089\ \text{GPa},\ SF_{\max} = 999,\quad \text{HEL} = 0.3\ \text{GPa},\ P_{\text{HEL}} = 0.25\ \text{GPa},$$

$$d_1 = 0.35,\quad d_2 = 0.5,\quad k_1 = 8.9\ \text{GPa},\quad k_2 = 0\ \text{GPa},\quad k_3 = 0\ \text{GPa},\quad FS = 0.15.$$

Since the focus is on the mechanical behavior of ice under dynamic loading, we calculated the damage parameters of ice D and the equivalent stress distributions $\sigma_{\text{eq}} = [(3/2)\sigma_{ij}\,\sigma_{ij} - (3p)^2]^{1/2}$ as a function of the loading duration. The calculations were performed for the model samples (see Fig. 1) using the above-cited consistent parameters under pulsed loading along the Z axis at a rate of 20 m/s. The results of calculations of the spatial-temporal distributions of D and σ_{eq} are presented in Fig. 2 for three time points 20, 50 and 75 μs from the onset of loading the sample. The intensity of sample coloring clearly demonstrates the evolution of the spatial distribution of the damage parameter D and the equivalent stresses σ_{eq} under vertical compression. In particular, as the time of sample compression increases, an increase is observed in the compressive stresses in the loading direction and in the tensile stresses in the radial direction. These stresses ensure the formation of a fully fractured ice zone and radial cracks in the central part of the sample. It is seen that as the time of dynamic compression increases, the number and depth of radial cracks increase. For the compression times 50 and 75 μs, there is a clear tendency towards formation of a synchronous bimodal (two-peak) spatial distribution of the damage parameter D and the equivalent stress σ_{eq}. The zone of volumetric damage, where the characteristic size of the fragments did not exceed that of the computational grid step, was formed on the contact surface between the sample and the mobile rigid wall. The propagation of this zone inwards the sample was accompanied by an increase in the characteristic fragment size and a formation of radial cracks.

Thus, the fracture in the sample loading conditions under study develops from the center towards the rear surface.

Let us look at the time variations of the stress of dynamic compression of ice, since these relationships play a decisive role in the applied field.

In the course of dynamic loading of the sample, the values of engineering strain $\varepsilon_{1\,\text{eng}}$ were calculated from the changes in the sample height calculated from the displacement of the mobile rigid wall

$$\varepsilon_{1\,\text{eng}} = \frac{1}{h_0}\int_0^t v(t)\,dt, \tag{6}$$

where h_0 is the initial sample height and $v(t)$ is the mobile wall velocity.

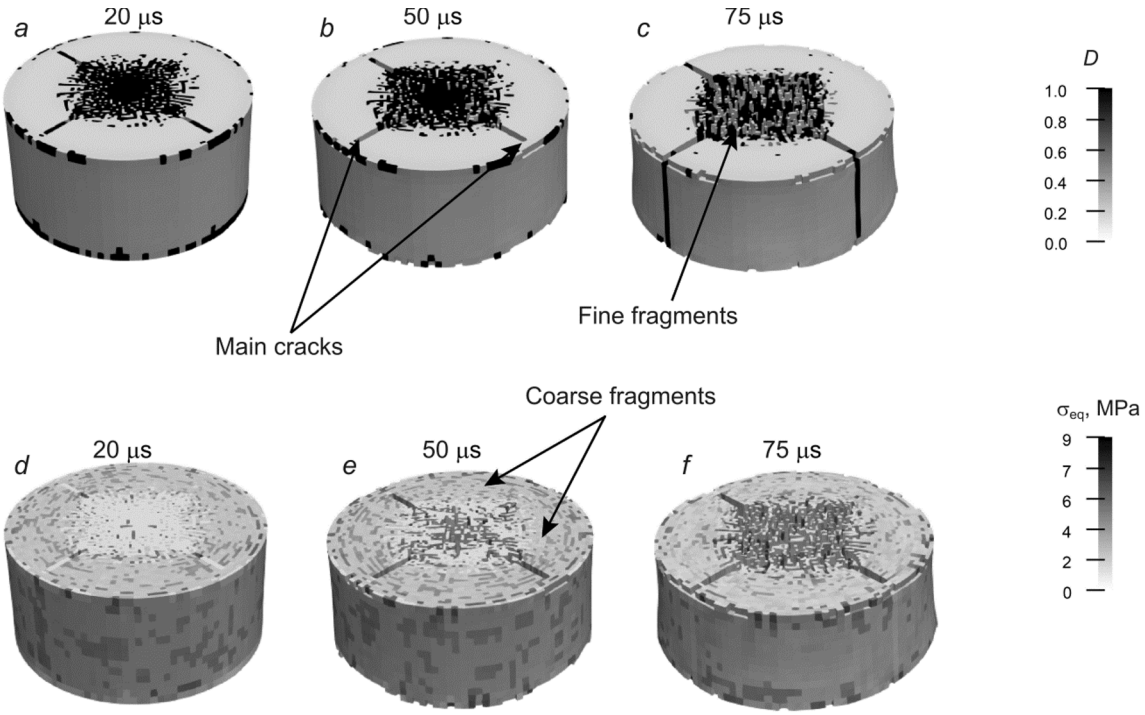

Fig. 2. Results of a numerical simulation of dynamic compression of ice: damage parameter D (*a–c*), equivalent stresses (*d–f*).

Considering the derived values of the engineering strain variation $\varepsilon_{1\,\mathrm{eng}}$, let us find the variation of the integral force of sample compression in time, which are recorded on the immobile wall, and the true strain variation in time in the form of

$$\sigma_{1\,\mathrm{true}} = (F(t)/\pi r^2)(1+\varepsilon_{1\,\mathrm{eng}}), \tag{7}$$

where $\sigma_{1\,\mathrm{true}}$ is the true strain, $F(t)$ is the force at the boundary with the immobile wall, and r is the sample radius at the boundary with the immobile wall.

The resulting numerical values of true strains in the course of deformation of a cylindrical sample under the conditions of high-rate axial compression are given in Fig. 3 in the form of a true strain versus time dependence in comparison with the experimental data [6, 26]. The values of true strain of Ih ice at a high strain rate (2000 s^{-1}) are in good qualitative and quantitative agreement. The absence of oscillations in the calculated true strain versus time curve is due to the use of the concepts of the surface erosion model [16, 27]. The fracture criterion is equivalent to condition (5). When the maximum equivalent inelastic deformation reaches its limit value in the mesh elements, these elements are thought to be fractured and are removed from the computational domain.

The calculated value of the specific absorbed energy under the assumed loading conditions was found to be 273.9 J/kg, while the experimentally obtained value was ~292.1 J/kg. The difference between the calculated and experimentally obtained values is less than 10%, which validates the adequacy of the model of high-rate deformation of Ih ice in the range of strain rates from 0.1 to 2000 s^{-1}.

To sum up, the proposed model and the physical-mechanical concepts of ice behavior under dynamic loading, discussed in this study ensure both qualitative and quantitative agreement of the results of mechanical behavior of Ih ice with the available experimental data and can be used to predict the results of high-velocity interaction of ice bodies and hail with the aircraft and structure elements of transport systems.

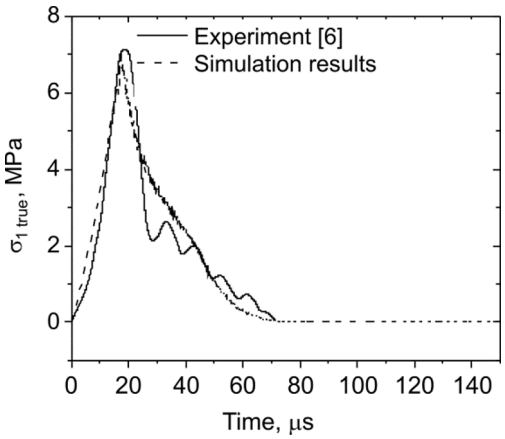

Fig. 3. True stress of axial compression versus time under dynamic compression of ice with a velocity amplitude of 20 m/s.

CONCLUSIONS

The mechanical behavior of ice under dynamic loading has been studied using Ih ice as an example. A computational model of the mechanical behavior of Ih ice under high-velocity impacts has been constructed. The mechanical behavior of ice under dynamic loading was described within the frame of the Johnson–Holmquist approach. The numerical values of model parameters of the mechanical behavior of ice were refined using the experimental data.

It has been shown that the proposed physical-mechanical concepts and the model ensure both qualitative and quantitative agreement of the results of mechanical behavior of Ih ice obtained in this study with the available experimental data in the range of pressures from 0 to 150 MPa at the temperatures from 193 to 273 K in the strain rate interval from 0 to 2000 1/s. This indicates the validity of the concepts used and allows predicting ice behavior under different dynamic loads.

This study was partially supported by the RFBR, Project No. 19-08-01152, and the Mendeleev Fund of the Tomsk State University.

REFERENCES

1. A. V. Shavlov, Ice in Structural Transformations [in Russian], Nauka, Novosibirsk (1996).
2. D. Saletti, D. George, V. Gouy, *et al*., Int. J. of Impact Eng., 132, 103315 (2019), DOI: 10.1016/j.ijimpeng.2019.103315.
3. J. Pernas-Sánchez, D. A. Pedroche, D. Varas, *et al*., Int. J. Solids Structur., **49**, No. 14, 1919 (2012), DOI: 10.1016/j.ijsolstr.2012.03.038.
4. Y. Wang, Y. Qin, and X. Yao, Appl. Ocean Res., 103, 102347 (2020), DOI: 10.1016/j.apor.2020.102347.
5. T. Sain and R. Narasimhan, Int. J. Solids Structur., **48**, No. 5, 817 (2011). 827, DOI: 10.1016/j.ijsolstr.2010.11.016.
6. A. Bragov, L. Igumnov, A. Konstantinov, *et al*., EPJ Web Conf., **94**, 01070 (2015), DOI: 10.1051/epjconf/20159401070.
7. E. Schulso, J. Phys. Colloq., **48**(C1), 207 (1987).
8. V. P. Glazyrin, Yu. N. Orlov, M. Yu. Orlov, and E. Yu. Poverennov, Izv. VUZov. Fiz., **55**, No. 9/3, 42 (2012).
9. V. P. Glazyrin, Yu. N. Orlov, M. Yu. Orlov, *et al*., Izv. VUZov. Fiz., **56**, No. 7/3, 38 (2013).

10. E. C. Hunke, Proc. IUTAM Symposium on Scaling Laws in Ice Mechanics and Ice Dynamics. Fairbanks, Alaska, U. S.A., 289 (2000).
11. J. Tuhkuri and A. Polojärvi, Philos. Trans. R. Soc. A, **376**, No. 2129, 20170335 (2018), DOI: 10.1098/rsta.2017.0335.
12. Yu. N. Orlov and M. Yu. Orlov, Tomsk State University Journal of Mathematics and Mechanics, **38**, 81 (2015).
13. P. G. Bergan, G. Cammaert, G. Skeie, and V. Tharigopula, IOP Conf. Ser.: Mater. Sci. Eng., **10**, 012102 (2010), DOI: 10.1088/1757-899x/10/1/012102.
14. M. Montagnat, O. Castelnau, P. D. Bons, *et al.*, J. Struct. Geology, **61**, 78 (Elsevier, 2013), DOI: 10.1016/j.jsg.2013.05.002.hal-01746108.
15. G. R. Johnson and T. J. Holmquist, AIP Conf. Proc., **309**, 981 (1994), DOI: 10.1063/1.46199.
16. LS DYNA keywords user's manual. Vol. II. Material models. 09/08/20 (r:13191) LS –DYNA R12. Livermore Software Technology, An Ansys Company.
17. N. K. Sinha, Cold Regions Sci. Technol., **17**, No. 2, 127 (1989), DOI:10.1016/s0165-232x(89)80003-5.
18. G. H. Shaw, J. Chem. Phys., **84**, No. 10, 5862 (1986), DOI: 10.1063/1.449897.
19. J. J. Petrovic, J. Mater. Sci., **38**, No. 1, 1 (2003), DOI: 10.1023/a:1021134128038.
20. J. J. Neumeier, J. Phys. Chem. Reference Data, **47**, No. 3, 033101 (2018), DOI: 10.1063/1.5030640.
21. S. T. Stewart and T. J. Ahrens, J. Geophys. Res.: Planets, **11**0, E03005 (2005), DOI: 10.1029/2004je002305.
22. R. Feistel and W. Wagner, J. Phys. Chem. Reference Data, **35**, No. 2, 1021 (2006), DOI: 10.1063/1.2183324.
23. T. Sain and R. Narasimhan, Int. J. Solids Structur., **48**, 817 (2011).
24. P. V. Makarov, M. O. Eremin, and A. Yu. Peryshkin, Izv. VUZov. Fiz., **56**, No. 7/3, 74 (2013).
25. Iv. S. Konovalenko, Ig. S. Konovalenko, A. Yu. Smolin, and S. G. Psahie, Izvestiya VUZov. Fiz., **56**, No. 7/3, 167 (2013).
26. S. Jones, J. Phys. Chem., **32**, 6099 (1997).
27. A. Pandolfi, B. Li, and M. Ortiz, Int. J. Fracture, **184**, Nos. 1–2, 3 (2012), DOI: 10.1007/s10704-012-9788-x.